Synthesis and Pressure Sensitive Adhesive Performance of Poly(EHA-*co*-AA)/Silicate Nanocomposite Used in Transdermal Drug Delivery

Pradeep K. Rana, Prafulla K. Sahoo

Department of Chemistry, Utkal University, Vani Vihar, Bhubaneswar 751 004, India

Received 26 March 2006; accepted 7 June 2007
DOI 10.1002/app.27034
Published online 4 September 2007 in Wiley InterScience (www.interscience.wiley.com).

ABSTRACT: The transdermal drug delivery (TDD) has got main advantage over the conventional oral delivery and maintaining the plasma drug level at a plateau over a long period of time. The phenomenon is taking place at the patch-skin interface, in particular the adhesion of a polymeric nanoscale pressure sensitive adhesive (PNPSA) film loaded with drug. The major requirements of this PNPSA are they should stick firmly to a difficult substrate (skin) and they should be easily and cleanly removed from the substrate when desired. The PNPSA nanocomposite P(EHA-*co*-AA)/SS is prepared by the emulsion copolymerization of two acrylic monomers, 2-ethyl hexylacrylate (EHA) and acrylic acid (AA) using a silicone additive like sodium silicate (SS). The TDD patch consists of a nanoscale silicone based polymeric adhesive i.e., P(EHA-*co*-AA)/SS and a drug Cloxacillin sodium an antibiotic. The prepared polymeric nanocomposites can carry drug and these bioactives are entrapped in the polymer matrix as particulates enmesh or bound to the particle surface by physical adsorption. The well characterized novel nanocomposites exhibited significant PSA performance in TDD system. In view of its medical application, the biodegradation study by activated sludge water indicated the nanocomposite to be environmentally friendly. © 2007 Wiley Periodicals, Inc. J Appl Polym Sci 106: 3915–3921, 2007

Key words: nanocomposite; pressure sensitive adhesion; drug delivery; biodegradation

INTRODUCTION

Silicate based polymers represent a new class of materials with high performance and is of great academic and industrial interests. The improved properties of these nanocomposites include mechanical,[1–4] thermal,[5,6] flammability[7,8] properties, and are related to the dispersion and nanostructure of the layered silicate in the polymer.

Pressure-sensitive adhesives (PSA) are used extensively in the pharmaceutical industry where the adhesive layers are used to adhere drug delivery devices, both active and passive patches, to the stratum corneum. PSAs are preferred as the adhesive in these systems because of their desirable properties of good initial and long-term adhesion, clean removability,[9] and skin and drug compatibility. In addition, their highly viscoelastic properties are necessary prerequisites for attachment to soft tissue. The interfacial adhesion and resistance to progressive debonding of the resulting adhesive/stratum corneum interface dominate the reliability of such transdermal devices. Adhesion and integrity of device function are governed by the polymer chemistry (choice of adhesive), layer thickness, content of additions (permeation enhancer and pharmaceutical loading), and environmental conditions (temperature, humidity, and physiological environment).[10] Somewhat surprisingly, the adhesion of PSAs is not well understood with almost no reproducible test methods or quantitative adhesion data. In particular, the trend toward increasingly complex and novel patch designs further necessitates the development of a systematic approach to quantify this adhesion.

In the medical field, silicone PSAs are used primarily in skin applications and particularly in transdermal drug delivery systems (TDDS). Medical grade silicone PSAs[11] can be released from liners much more easily than their industrial counterparts, as they are formulated to be less aggressive. Many manufacturers prefer silicon adhesives,[12] because they are kind to the skin. They are also chemically stable, biologically inert, and transparent, retain adhesive properties in the presence of moisture, and have high permeability. One of the most important properties of an adhesive to be used in medical applications is biocompatibility (nontoxic).[13]

Acrylic polymers currently dominate the other pressure sensitive medical markets, because of their

Correspondence to: P. K. Sahoo (psahoochemuu@satyam.net.in).

Contract grant sponsor: University Grants Commission, New Delhi, India; contract grant number: MR Project No.F.12-79/2001(SR-II).

Journal of Applied Polymer Science, Vol. 106, 3915–3921 (2007)

low level of allergenicity. Acrylic PSAs are designed for skin clean removal, low odor, low rates of chemical and mechanical irritation, and acceptance resistance to cobalt and ethylene oxide sterilization.

Acrylic monomer based conventional emulsion polymerization were reported previously by different authors[14–17] with the highlight of adhesion and mechanical properties. The bioadhesion offered by nanoparticles[18] could be attributed to several factors like an increase of the adhesive force due to decrease in size (nanoscopic). In our previous article[4] we report the synthesis and characterization of intercalated homopolymer/silicate nanocomposites (PEHA/SS), but it fails to exhibit TDD property. As a result we are tempted to prepare a copolymer based nanocomposite that shows remarkable adhesion in TDDS. In this article we have illustrated a new concept of a polymeric silicate based nanocomposite, i.e., P(EHA-*co*-AA)/SS to act as a PSA in TDD. Acrylic acid (AA) was taken for its polarity and known bioadhesive properties and EHA was taken for hydrophobicity and fluidity to act as a plastisizer within the copolymer.

EXPERIMENT

Materials

Monomers, 2-ethyl hexylacrylate (EHA) and acrylic acid (AA) were purchased from SRL India and cloxacillin sodium was purchased from Emerck, Germany; benzoyl peroxide (BPO) from Himedia India and sodium silicate (SS) was a gift sample from PQ Corporation, Netherlands.

Preparation of nanocomposite

Distilled EHA and AA were dispersed (v/v ratio as shown in Table I) in deionized water via stirring with sorbitol (surfactant). Silicate solution was prepared by weight percentage basis [2% (w/v) SS] for the suitability of the experiment. The mixture was slowly heated to 80°C and the initiator BPO was added as per suitability of the polymerization. Emulsion polymerization was carried out with a constant stirring speed at 80°C. After 2 h of reaction, the drug cloxacillin sodium was added on weight percentage basis. After a total of 3 h of reaction, polymerization was terminated by the addition of a 0.1*M* solution of ferrous ammonium sulfate solution. The coagulated products were purified by washing with distilled water and other solvents and then dried at 45°C.

Characterization

The entrapping of the drugs into the nanocomposite i.e., P(EHA-*co*-AA)/SS was investigated by means of transmission electron microscopy (TEM) (H-7100, Hitachi), operated at an accelerating voltage of 100 kV. The ultra thin section (the edge of the sample sheet perpendicular to the compression mold) with a thickness of 100 nm was microtomed at −80°C.

TABLE I
Monomer Composition Ratio and Corresponding Adhesive Forces at Contact Time 60 s

Sample code	Monomer ratio (EHA : AA)	Force in mN/cm^2 on		
		Glass	Steel	Skin
S1	100 : 00	317.16	289.56	22.77
S2	80 : 20	319.78	266.37	26.63
S3	60 : 40	330.34	315.45	31.18
S4	50 : 50	303.67	295.68	38.26
S5	40 : 60	389.19	367.18	44.72
S6	20 : 80	460.62	432.37	26.33
S7	00 : 100	245.31	217.19	15.12

The H^1-NMR of the composite P(EHA-*co*-AA)/SS was measured at temperature 296 K with a Jeol, GSX 400 with 250 Hz/cm using THF (deuterated) as the solvent.

The IR spectra of PEHA, PAA, P(EHA-*co*-AA), and P(EHA-*co*-AA)/silicate in form of KBr pellets were recorded in the Perkin-Elmer model Paragon-500 FTIR spectrophotometer for proof of copolymerization.

Thermal properties were measured by using a Shimadzu DTA-500 system. It was carried out in air, from room temperature to 600°C at a heating rate of 10°C/min.

Water absorbency

As mentioned in our previous article.[4]

Peeling test

As mentioned in our previous aricle.[4]

Biodegradation

Degradation by activated sludge

The activated sludge water was collected from septic tank receiving toilet and domestic wastewater. The sludge was collected[19] in a polypropylene container, which was filled completely and was then closed perfectly. Then the wastewater was brought to the lab immediately. After settling for about 1 h the total solid concentration was increased to 5000 mg/L. The activated sludge water and a polymer sample (0.2 g) were incubated together in a sterilized vessel at room temperature (28 ± 2)°C. Duplicate samples were removed at time intervals for biodegradation study via weight loss. Vessels containing polymer samples without sludge water were treated as control.

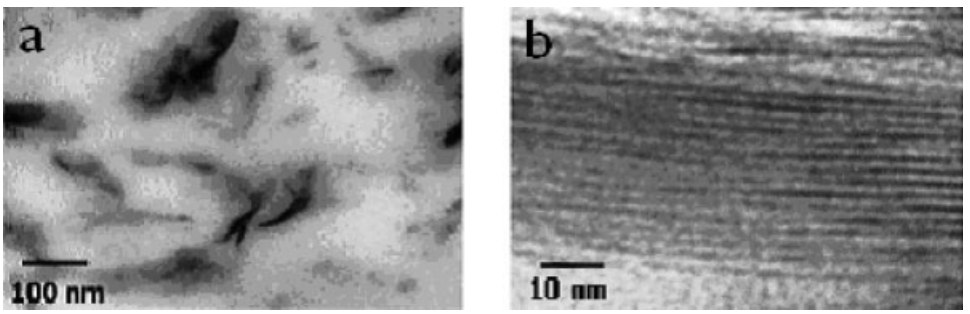

Figure 1 TEM of (PEHA-*co*-AA)/SS composites at 100 nm (a) and 10 nm (b) intensity.

Degradation in cultured medium

A cultured medium was prepared by taking nutrient broth. In those medium *E.coli* bacteria was inoculated. The pure culture was maintained separately in the incubator. The nutrient broth so prepared was sterilized for 45 min at a pressure of 15 lb/in^2 at 80°C. Then to 10 mL of sterilized broth, 0.1 g each of the samples i.e., PEHA, PAA, and P(EHA-*co*-AA)/SS samples were added asceptically in separate test tubes, and each tube of samples were supplemented with inoculome of the bacterial strains separately.

The degradation of samples by *E.Coli* was monitored in time intervals of 1, 8, 15 and 30 days. After the required time period the samples were washed repeatedly with deionized water, oven dried at (40 ± 1)°C for 24 h. Then the samples were weighed to determine the weight loss. Biodegradation through *E.Coli* was studied by the amount of CO_2 evolved[20] during the incubation periods of 1, 8, 15, and 30 days.

Quantitative estimation of free CO_2

Chemicals requirement: Na_2CO_3, phenolphthalein indicator.

Procedure: The cultured sample (''*X*'' mL) and blank tube was titrated against Na_2CO_3 (N/50) (''*Y*'' mL) using phenolphthalein indicator until the pink color persists for at least 30 s. This was continued till getting a concordant reading.

Calculation:

$$N_1V_1 = N_2V_2$$
$$(CO_2) \quad (Na_2CO_3)$$
$$\Rightarrow N_1 \times X = (1/50) \times Y$$
$$\Rightarrow \text{Strength} = (Y \times 22)/(50 \times X)$$
$$\Rightarrow \text{Free } CO_2 = [(Y \times 22 \times 1000)/(50 \times X)]\text{mg}/l$$
$$\Rightarrow \text{Free } CO_2 = [(440 \times Y)/X]\text{ppm}.$$

RESULTS AND DISCUSSION

Transmission electron microscopy

The dispersion microstructure of the intercalated silicate layers is being examined by means of TEM. TEM image of P(EHA-*co*-AA)/silicate (Fig. 1) demonstrates that the silicate layers are structured in good order, and are well dispersed in the polymer matrix.[21] The periodic alternating dark and light bands represent the layers of silicate and interlayer, respectively. The smaller interlayer spacing in the figure indicates the intercalation not exfoliation. This is in good agreement with our previous report.[4] The space produced by the intercalated silicate layers, may be engaged by the entrapped drugs in the polymer matrix and also adsorbed onto the surface of the nanoparticles. So the drug molecules may be physically adsorbed only on the polymer surface. Finally, the images confirm that the synthesized composite is a nanoscale material and the particle size is found to be 10 nm (at low magnification) and 100 nm (at high magnification).

X-ray diffraction

From XRD pattern of the polymers, the *d*-spacings are calculated from Bragg formula, at peak positions. Because of the intercalation of P(EHA-*co*-AA) into the galleries via emulsion polymerization, the *d*-spacing of P(EHA-*co*-AA)/silicate nanocomposites increases from 1.85 nm to 2.62 nm in the dry state, even though the interlayer distances of the PEHA/silicate exhibits small deviation (Fig. 2). This is a strong indication that there is no trace for the occurrence of the delamination or exfoliation. The XRD patterns suggest that sample P(EHA-*co*-AA) with the drug is being inserted into the galleries of the hydrophilic silicate through emulsion polymerization.[22]

Nuclear magnetic resonance (H^1)

From the H^1-NMR spectra of the sample P(EHA-*co*-AA), the absence of any peak at 5–6 ppm indicates that the copolymer is completely pure (i.e., without any impurities) as shown neatly in Figure 3. The peaks are explained below.

(a) For EHA, the peaks appear at 0.85–2.25 ppm and also at 3.9 ppm. Peaks for two —CH_3

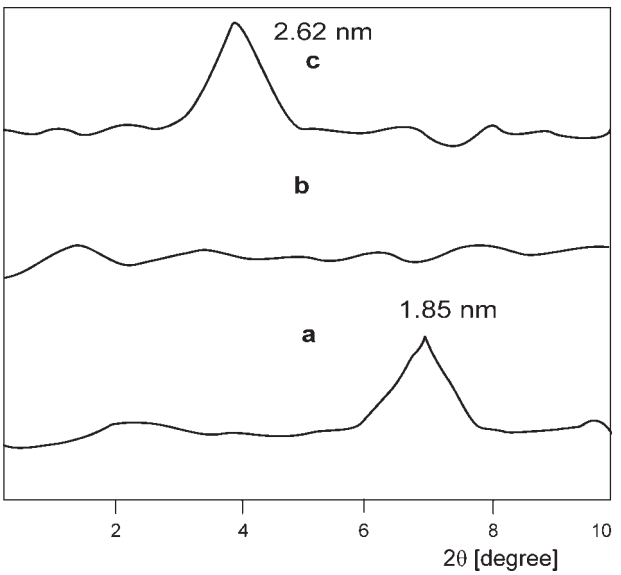

Figure 2 XRD curve of (a) sodium silicate, (b) P(EHA-*co*-AA), and (c) P(EHA-*co*-AA)/silicate.

groups appear at 0.85 and 0.91 ppm and peaks for fourth —CH_2 group and one methine proton appear at 1.28 and 1.40 ppm, respectively. The protons of backbone vinyl group, (i.e., for methylene and methine) show peaks at 1.55 and 2.25 ppm, respectively. The peak for the pendant —CH_2 group appears at 3.9 ppm.

(b) For the AA, a doublet peak is found at 1.1 ppm for —CH_2 group, a triplet at 1.9 ppm for methine group of the backbone and a weak peak appears at 12.1 ppm for the carboxylic proton.

Hence, the H^1-NMR spectra shown in Figure 3 confirms the formation of the copolymer i.e., P(EHA-*co*-AA).

FT infrared

Figure 4 shows comparative FTIR spectra of PEHA, PAA, and P(EHA-*co*-AA). Absorption bands at 1545, 1406, and 1015 cm^{-1}, assigned to the carbonyl group of the carboxylate of PEHA [Fig. 4(a)]. In PAA [Fig. 4(b)], peak at 1715 cm^{-1} is due to —COOH acid group. The absence of absorption peak at 1630 cm^{-1} region due to C=C bond confirms the absence of monomer impurities in the copolymer. For the

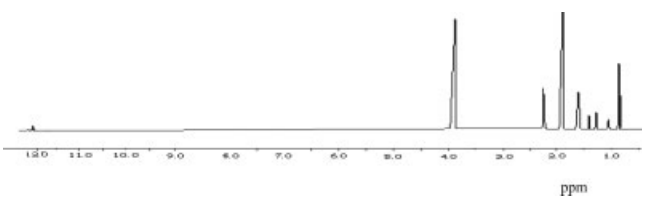

Figure 3 H^1-NMR spectra of P(EHA-*co*-AA) with a monomer feed ratio of 40 : 60.

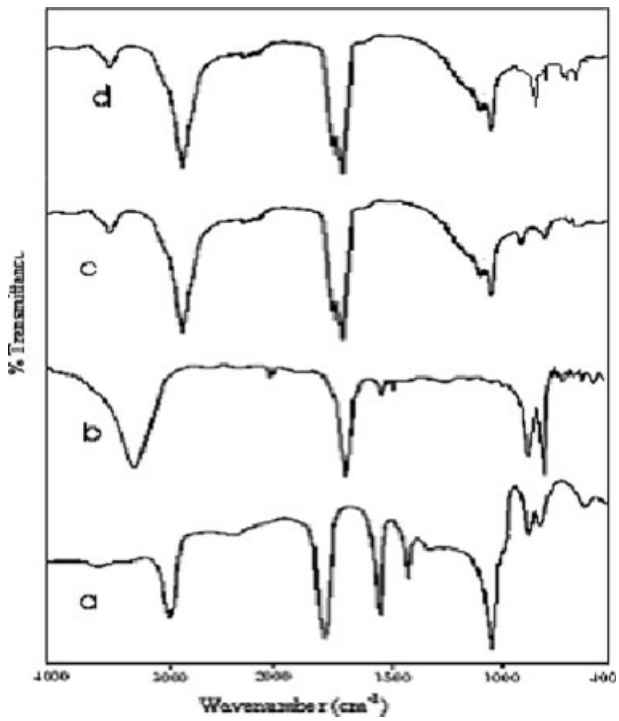

Figure 4 FTIR spectra of (a) PEHA, (b) PAA and (c) P(EHA-*co*-AA).

copolymer, P(EHA-*co*-AA) as shown in the Figure 4(c), the characteristic peaks for both EHA and AA are present with little shifting of position. Again the presence of peak in the region 618 cm^{-1} and 900–1100 cm^{-1} confirms that there is Si—O—Si bonding due to silicate in the polymer matrices.

Thermogravimetry analysis

The thermal behaviors of PEHA, PAA, and P(EHA-*co*-AA) are studied at room temperature at 28°C by comparing their thermogram (TGA) curves as shown in Figure 5. From the curves, the temperatures of

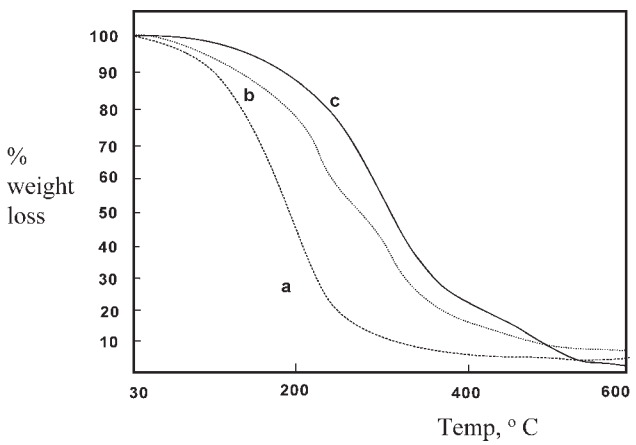

Figure 5 TGA thermogram of (a) PEHA, (b) PAA and (c) P(EHA-*co*-AA)/SS.

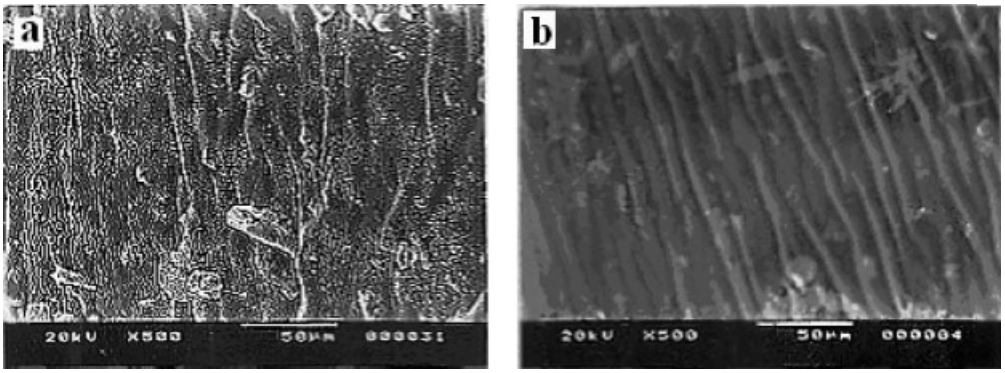

Figure 6 SEM of P(EHA-*co*-AA)/SS before (a) and after (b) biodegradation.

decomposition (T_D) are found to be 130°C for PEHA, 185°C for PAA, and 225°C for P(EHA-*co*-AA)/SS. The nanocomposites P(EHA-*co*-AA)/SS exhibit higher thermal stability because of the higher decomposition onset temperature than that of PEHA and PAA, which can be attributed to the nanoscale entrapment of drugs and silicone penetration onto the matrix.

Scanning electron microscopy

A standard method for the observation of surface morphology is the scanning electron microscopy (SEM). From Figure 6 it is clear that the roughness of the surface is mostly communicating with large amount of silicates in the mixture, making the polymer matrix more porous. Further, the SEM of the P(EHA-*co*-AA)/SS before and after biodegradation clearly confirmed the extent of biodegradability as the roughness of the surface in Figure 6(a) became plane in Figure 6(b) due to the microorganism growth.

Peel adhesion study

The nanocomposites exhibit good performances as pressure sensitive tapes on glass, steel, and skin (Table I). It shows better result as a PSA for higher energetic surfaces like glass and steel. The carbonyl group present in it plays an important role in adhesion with the surface. The forces of adhesion obtained on wet glass and steel surfaces show no correlation with those obtained in contact with skin, as wet glass and steel surfaces are not an appropriate substrate for force of adhesion determination. This may be due to the fact that the glass and steel surfaces are completely flat and hard and thus the initial contact with such surfaces is very different than that with soft tissue.

The S_5 sample shows good adhesion over skin than any other monomer feed ratio samples. This is ascribed to the increase of the AA feed ratio enhancing the hydrophilicity of the PSA film; as a result, it can bind the skin more easily than other samples. Upon contact with the skin, a good force of adhesion is created at the interface, which requires a greater tensile strength to break the bond. But after this ratio (EHA : AA :: 40 : 60), the tacking nature of the polymer decreases, due to more water holding capacity of the sample.

Drug release study (dissolution method)

About 3% (w/w) of drug, cloxacillin Sodium, an antibiotic, in three films of different thickness (i.e., about 100, 150, and 200 μm) are prepared for these experiments on 300 μm thick skin. Stabilized adhesion methodology is used with a period of 1 h between each application. Results are reported in Figure 7. During adhesion, it is found that for 100 μm thick film the drug release is stable, 1.1–1.45 μg/cm^2. For 150 μm thick film, the drug release is moderate, 1.2–2.2 μg/cm^2, and for 200 μm thick film, the drug release study shows an interesting result, 1.5–3.9 μg/cm^2 i.e., there is a large increase in drug release during both 2nd and 3rd h and then a stable curve is obtained. This is explained on the fact that the increase of the film thickness is the reason for higher quantities of drug release.

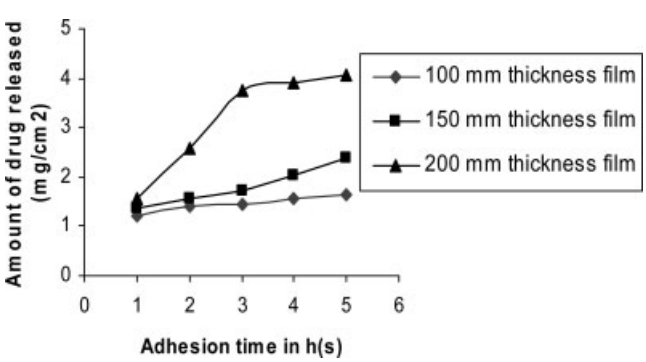

Figure 7 Drug release in the skin in adhesion time intervals for films of various thicknesses.

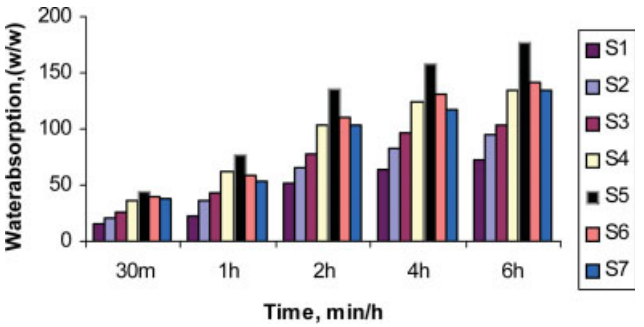

Figure 8 Water absorption of P(EHA-*co*-AA)/SS (SS_{1-7}). [Color figure can be viewed in the online issue, which is available at www.interscience.wiley.com.]

Water absorbency

From Figure 8, it is found that on increasing the monomer (AA) content in the copolymer, the water absorbency increases and then gradually decreases. The increase of water absorbency from S_1 to S_5 is due to the fact that the hydrophilic part of the polymer enhances the water absorption, and also SS plays an important role i.e., as a crosslinker to increase the water content by forming large number of rooms in the composite. But from S_5 to S_7 the samples shows a decreased trend of biodegradation, as the formation of excess of crosslinked density, which results in the less water absorption due to the unavailability of free space in the composite.

Biodegradation by activated sludge, *E.Coli*, and Quantitative estimation of CO_2

From the comparative biodegradation study of PEHA, PAA, P(EHA-*co*-AA) and P(EHA-*co*-AA)/SS, it was found that PAA showed accelerated rate of degradation (by weight loss). But P(EHA-*co*-AA)/SS

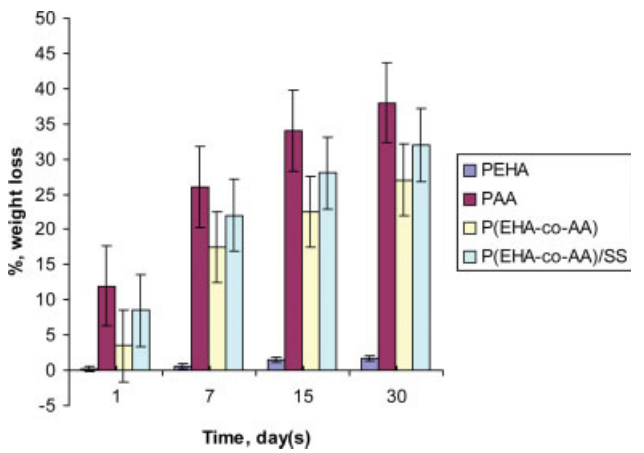

Figure 9 Biodegradation of PEHA, PAA, P(EHA-*co*-AA), and P(EHA-*co*-AA)/SS by activated sludge measured by weight loss. [Color figure can be viewed in the online issue, which is available at www.interscience.wiley.com.]

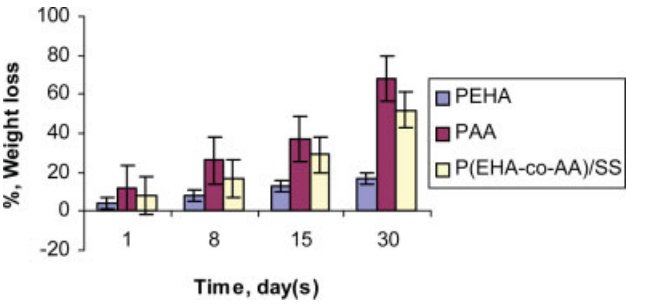

Figure 10 Biodegradation of PEHA, PAA, and P(EHA-*co*-AA)/SS by *E.coli* measured by weight loss. [Color figure can be viewed in the online issue, which is available at www.interscience.wiley.com.]

showed more amount of weight loss than in case of PEHA and P(EHA-*co*-AA) as shown in Figure 9. As P(EHA-*co*-AA)/SS has more net like space than others, it holds up more water, as a result of which it is more biodegradable.

Biodegradation by *E.coli* is studied for PEHA, PAA, and P(EHA-*co*-AA)/SS. At first, the degradation is calculated from the amount of weight loss after different periods of incubation i.e., 1, 8, 15, 30 days as shown in Figure 10. It is clearly visible that PAA degrade more than PEHA and P(EHA-*co*-AA)/SS, because the former is hydrophilic, hence absorbs more water in its network and facilitates the bacteria to grow up rapidly, thus enhancing the biodegradation. On the other hand, due to the hydrophobic nature of PEHA and P(EHA-*co*-AA)/SS the water absorbency is less, which, in turn, results in less biodegradation.

Again, from Figure 11, the amount of CO_2 released from different samples i.e., PEHA, PAA, and P(EHA-*co*-AA)/SS, confirms that biodegradation of the composite occurs moderately and can be possible in the environmental conditions too. However, the order of biodegradation for both the methods of determination is as follows: PAA > P(EHA-*co*-AA)/SS > PEHA.

The precise schematic illustration of the article has been represented in the Figure 12 below.

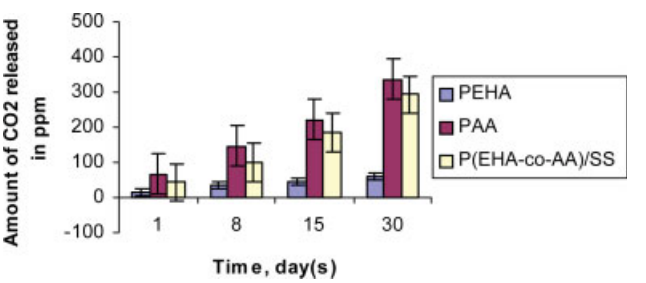

Figure 11 Biodegradation of PEHA, PAA, and P(EHA-*co*-AA)/SS by *E.coli* measured by CO_2 evolved. [Color figure can be viewed in the online issue, which is available at www.interscience.wiley.com.]

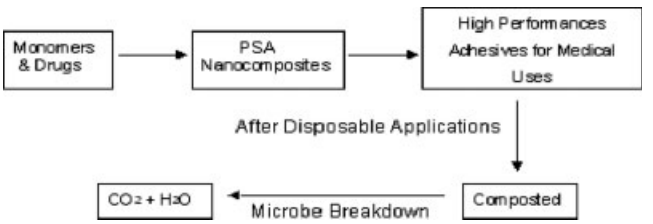

Figure 12 Schematic illustration of the concept of the article.

CONCLUSIONS

Novel P(EHA-*co*-AA)/SS nanocomposite PSA was prepared by emulsion technique with layer silicate. The TEM showed the well dispersion of the polymer nanocomposite into the intercalated silicate layers and the drug molecule may be adsorbed physically in the nanocomposite. The novel nanocomposite was further characterized by NMR, IR, TGA, and exhibited excellent properties of higher thermal stability, pressure sensitive adhesion, and superabsorbency for use as high performance materials. In view of their commercial application, the study of their biodegradability became important and those in sludge water show better degradation by microorganism at moderate silicate additive than the PEHA and P(EHA-*co*-AA) without silicate. The biodegradation and PSA performance of these nanocomposites in TDDS signified increased importance as environmentally friendly biomedical materials.

References

1. Wang, Z.; Pinmavaia, T. J Chem Mater 1998, 10, 820.
2. Burnside, S. D.; Giannelis, E. P. Chem Mater 1995, 7, 1597.
3. Giannelis, E. P. Adv Mater 1996, 8, 29.
4. Rana, P. K.; Swain, S. K.; Sahoo, P. K. J Appl Polym Sci 2004, 93, 1007.
5. Wang, W.; Hu, Y.; Song, L.; Chen, Z.; Fan, W. Polym Degrad Stabil 2002, 77, 423.
6. Gilman, J. W.; Jackson, C. L.; Morgan, A. B.; Harris, R. Chem Mater 2000, 12, 1866.
7. Gilman, J. W. Appl Clay Sci 1999, 15, 31.
8. Beyer, G. Plastics Additives Compounding, 2002, 4, 22.
9. Hendrics, J. O.; Dahlquist, C. A. Adhesion and Adhesives, 2nd ed.; Elsevier: London, UK, 1967.
10. Venkatraman, S.; Gale, R. Biomaterials 1998, 19, 1119.
11. Gopinath, L. Chem Br 1997, 33, 32.
12. Salin, D. G. M.; Becourt, P.; Couarraze, G. Int J Pharm 2000, 200, 121.
13. Stausberg, R. L.; Link, R. P. Tibech, 1990, 5.
14. Sandardi, F.; Zubir, A. J Macromol Sci Chem A 1985, 22, 1647.
15. Xu, Z.; Lu, G.; Cheng, S.; Li, J. J Appl Polym Sci 1995, 56, 575.
16. Zurkova, E.; Bouchal, K.; Zdenkova, D.; Pelzbauer, Z.; Svec, F.; Kalal, J. J Polym Sci: Polym Chem 1983, 21, 2949.
17. Okubo, M.; Nakamura, Y.; Matsumoto, T. J Polym Sci: Polym Chem Ed 1980, 18, 2451.
18. Vyas, S. P.; Khar, R. K. Targeted and Controlled Drug Delivery Novel Carrier Systems, 1st ed; CBS Publishers: New Delhi, India, 2002.
19. Federle, T. W.; Barlaz, M. A.; Pettigrew, C. A.; Kerr, K. M.; Kemper, J. J.; Nuck, B. A.; Schechtman, L. A. Biomacromolecules 2002, 3, 813.
20. Vermani, O. P.; Narula, A. K. Applied Chemistry (Theory and Practical); Wiley Eastern: New Delhi, India, 1989.
21. Morgan, A. B.; Gilman, J. W. J Appl Polym Sci 2003, 87, 1329.
22. Noh, M. W.; Lee, D. C. Polym Bull 1999, 42, 619.